

Knowledge Distillation on Spatial-Temporal Graph Convolutional Network for Traffic Prediction

Mohammad Izadi^a, Mehran Safayani^{a,*}, Abdolreza Mirzaei^a

^a*Department of Electrical and Computer Engineering, Isfahan University of Technology, Isfahan 84156-83111, Iran*

Abstract

Efficient real-time traffic prediction is crucial for reducing transportation time. To predict traffic conditions, we employ a spatio-temporal graph neural network (ST-GNN) to model our real-time traffic data as temporal graphs. Despite its capabilities, it often encounters challenges in delivering efficient real-time predictions for real-world traffic data. Recognizing the significance of timely prediction due to the dynamic nature of real-time data, we employ knowledge distillation (KD) as a solution to enhance the execution time of ST-GNNs for traffic prediction. In this paper, We introduce a cost function designed to train a network with fewer parameters (the student) using distilled data from a complex network (the teacher) while maintaining its accuracy close to that of the teacher. We use knowledge distillation, incorporating spatial-temporal correlations from the teacher network to enable the student to learn the complex patterns perceived by the teacher. However, a challenge arises in determining the student network architecture rather than considering it inadvertently. To address this challenge, we propose an algorithm that utilizes the cost function to calculate pruning scores, addressing small network architecture search issues, and jointly fine-tunes the network resulting from each pruning stage using KD. Ultimately, we evaluate our proposed ideas on two real-world datasets, PeMSD7 and PeMSD8. The results indicate that our method can maintain the student's accuracy close to that of the teacher, even with the retention of only 3% of network parameters.

Keywords: Traffic prediction, Spatial-temporal graph knowledge distillation, Spatial-temporal graph neural network pruning, Model compression, Teacher-student architecture

*Corresponding author.

Email addresses: m.izadi@ec.iut.ac.ir (Mohammad Izadi), safayani@iut.ac.ir (Mehran Safayani), mirzaei@iut.ac.ir (Abdolreza Mirzaei)

1. Introduction

Traffic prediction is a critical task in urban planning, logistics, and transportation management Yu et al. (2018); Tedjopurnomo et al. (2022). The data necessary for accurate prediction is typically sourced from monitoring stations strategically positioned throughout urban areas. These stations continuously collect a plethora of traffic-related parameters, including vehicle speed, traffic density, and flow rates, at regular intervals. This data is then structured into temporal graphs, with each node representing the traffic conditions observed at a specific monitoring station, and the edges indicating the connections between these stations Yu et al. (2018); Jiang and Luo (2022). To leverage this wealth of data for predictive purposes, spatio-temporal graph neural networks (ST-GNNs) have emerged as a promising approach. These networks have the capability to analyze the temporal evolution of traffic patterns and make accurate predictions regarding future traffic conditions for each monitoring station within desired time intervals. However, a significant challenge arises when dealing with a large number of nodes, as it can lead to computationally expensive operations and demand substantial hardware resources Yu et al. (2018).

In response to this challenge, our research focuses on enhancing the execution time of ST-GNNs through the application of an integrated algorithm that combines knowledge distillation and network pruning Hinton et al. (2015); Zhang et al. (2019); Meng et al. (2019); Passban et al. (2021); Wang et al. (2020); Li et al. (2024); Ji et al. (2022); Li et al. (2022); Jiang and Luo (2022); Molchanov et al. (2019).

Previous works have not implemented an integrated algorithm to address the structure search for student networks by considering the capability of learning by filters using knowledge distillation. These studies typically consider the student structure static, or those that do address structure search for finding student structures do not mention using knowledge distillation to address the capability of filters to learn from the teacher. Instead, they simply use task-specific cost functions. In contrast, we address both aspects within a single algorithm, integrating them seamlessly in one training phase. Our approach uses knowledge distillation to train a simplified "student" network with fewer parameters, helping it to understand complex spatial and temporal data by learning from a more complex "teacher" network. To refine the student network's architecture, we introduce a pruning algorithm that scores the capability of student filters in learning this information. Insignificant parameters are eliminated, and after each pruning stage, we fine-tune the network using knowledge distillation. This iterative process enhances the student network's efficiency and learn-

ing capability, leading to improvements in execution time without compromising accuracy Hinton et al. (2015); Gou et al. (2021); Cheng et al. (2020); Yim et al. (2017); Yang et al. (2021). By integrating pruning and knowledge distillation, our method effectively addresses the dual challenge of structuring student networks and enhancing their ability to learn complex data from the teacher model, resulting in a streamlined and effective training process.

The evaluation of our proposed approach is conducted using real-world traffic datasets, PeMSD7 and PeMSD8. Our results demonstrate that the student network trained using our cost function outperforms previous approaches in terms of both knowledge distillation effectiveness and execution time reduction. By jointly applying knowledge distillation and pruning, we assess the competency of network parameters, ensuring efficient model compression without sacrificing predictive accuracy. The structure of the paper is organized as follows: Section 2 explores related works on knowledge distillation, network pruning, and spatio-temporal graph neural networks. Section 3 introduces a ST-GNN model and the proposed knowledge distillation methods. It also discusses a pruning algorithm designed to address challenges in the student network architecture. Section 4 evaluates the performance of various cost functions on the PeMSD7 and PeMSD8 datasets, presenting ablation studies and analyzing their results. Finally, Section 5 outlines future works and draws conclusions.

2. Related Works

2.1. Traffic Prediction and Spatio-Temporal Graph Neural Networks

Fast and accurate urban traffic prediction is vital for traffic control and management, especially for medium and long-term forecasts. Traditional methods often struggle with complexities in traffic flow and neglect spatial and temporal dependencies. To address this, deep networks capable of handling such data have been proposed.

In Ramakrishnan and Soni (2018), the significance of traffic network prediction and its applications, such as network monitoring, is discussed. Various recurrent neural network architectures, including standard RNN, LSTM, and GRU, are explored for traffic prediction. However, these models suffer from high execution times and difficulties in capturing long-range dependencies due to numerous parameters.

Bidirectional LSTM models are found to outperform unidirectional LSTM models in Abduljabbar

et al. (2021), offering improved accuracy. Despite this, the high computational cost remains a significant drawback, making these models less suitable for real-time applications.

Spatio-temporal graph neural networks (ST-GNNs) are introduced to address these limitations by utilizing graph convolution layers for spatial processing and convolution layers for capturing temporal correlations. This approach offers reduced execution time and comparable or better accuracy. In Guo et al. (2019), the attentional spatio-temporal graph convolutional network (ASTGCN) model effectively predicts traffic flow by leveraging spatial-temporal attention mechanisms and convolution layers. However, the model complexity and training time can still be high.

The spatio-temporal graph convolutional networks (STGCN) framework presented in Yu et al. (2018) shows enhanced training efficiency and captures comprehensive spatial-temporal correlations, outperforming other methods on real traffic datasets. Yet, it still faces challenges in scaling to very large networks and handling diverse urban environments.

Recent surveys such as Jiang and Luo (2022) and Jiang et al. (2023) provide comprehensive overviews of advancements in this field, highlighting the progress and persistent challenges such as handling heterogeneous data sources and improving model interpretability.

2.2. Knowledge Distillation

Knowledge Distillation, or *Teacher-Student Learning*, introduced in Hinton et al. (2015) in 2015, transfers knowledge from a complex "teacher" network to a smaller "student" network. This alignment of behavior and predictions improves student performance and reduces computational resources.

Further research extends this to graph and spatio-temporal networks. In Yang et al. (2020), a novel approach for knowledge transfer from a GCN teacher model to a GCN student model is introduced, leading to a smaller model with improved execution time, particularly suited for dynamic graph models. However, this method may struggle with the heterogeneity of traffic data.

In Jing et al. (2021), the objective is to train a simpler network through knowledge distillation from multiple GCN teacher models with different tasks, extending to distill spatial graph information from hidden convolutional layers. This approach empowers the student model to excel in various tasks without additional labeled data, but the integration of heterogeneous knowledge remains challenging.

In Bian et al. (2021), knowledge distillation is extended to ST-GNNs for modeling spatial and tem-

poral data in human body position videos, utilizing various techniques, including minimizing loss, leveraging spatial-temporal relations, and using the gradient rejuvenation method to optimize the student model. Despite its success, adapting this approach to the diverse and dynamic nature of urban traffic data poses significant challenges.

2.3. Pruning and Fine-Tuning

In 1990, neural network pruning was first introduced by LeCun et al. (1989), offering a method to identify connections safe for pruning using the Hessian matrix. This reduces parameters in large networks, mitigating overfitting and resource requirements, crucial for deployment on constrained devices. Pruning has since become essential for compressing networks across diverse applications. In 2019, Molchanov et al. (2019) proposed a method to estimate layer and weight importance, facilitating the removal of unimportant weights and network size reduction. Iterative pruning and retraining stages improve performance and reduce model complexity. However, maintaining performance while significantly reducing model size remains a persistent challenge.

3. Proposed Methods

Traffic prediction, involves predicting future values of key traffic conditions (e.g., speed or traffic flow) for the next h time steps based on M prior traffic observations. In this paper, we model the traffic network as graphs defined across time steps. At time step t , data from N monitoring stations is represented as a graph $G_t = (V_t, E, W)$, where $V_t \in \mathbb{R}^N$ contains features from N nodes (e.g., road segments) with speed as the chosen criterion. The edge set E depicts connections between stations, defined based on distance criteria, reflecting the influence of stations on each other. Weights $W \in \mathbb{R}^{N \times N}$ in the weighted adjacency matrix signify the relationships between stations, often determined by spatial disparities.

The ST-GCNYu et al. (2018), designed for traffic prediction, processes spatial and temporal data. Graph convolution layers capture spatial relationships and node features over time. Convolutional layers model temporal correlations, focusing on sequential patterns and changes between graphs. The architecture comprises two blocks with temporal and spatial layers, and an output block transforms information into the final output. The teacher and student networks share an identical number of blocks and layers. Any variations in parameters result from differences in channel numbers within the temporal and spatial layers of the hidden layer. The complex ST-GCN teacher

network achieves high accuracy with 333,604 and 296,426 parameters for PeMSD7 and PeMSD8 datasets (Table 1 and Figure 1). Despite accuracy, its high parameter count results in significant computational cost (see Table 1, first row). A proposed lighter model, the student network (see Table 1, third row) is a scaled-down version of the teacher network. With 10,144 and 7,766 parameters for PeMSD7 and PeMSD8, it maintains accuracy while reducing complexity and computational requirements. This lightweight solution is efficient for traffic prediction, especially in resource-constrained scenarios.

3.1. Knowledge Distillation

In this paper, we use offline distillation, wherein the student distills information from the teacher network after the teacher network has been completely trained Asif et al. (2020); Mirzadeh et al. (2020); Mobahi et al. (2020). We utilized two knowledge distillation techniques. The initial approach, known as response-based distillation, involves transmitting crucial information from the teacher network’s outputs to the student network. This leads to the development of a simpler and faster model while simultaneously preserving performance. The second method, feature-based knowledge distillation, focuses on hidden layer’s knowledge, encompassing spatial and temporal correlations among graph nodes (Figure 1).

Table 1: Network information for knowledge distillation and pruning

PeMSD7				
Models	Parameters	Hidden Blocks Channel	Test Time (s)	FLOPS
Teacher	333,604	[1, 32, 64][64, 32, 128]	3.423	49,889,172,087
Pruning Base Model	48,628	[1, 8, 16][16, 8, 32]	1.069	9,113,934,711
Student	10,144	[1, 2, 4][4, 2, 8]	0.547	1,726,990,455

PeMSD8				
Models	Parameters	Hidden Blocks Channel	Test Time (s)	FLOPS
Teacher	296,426	[1, 32, 64][64, 32, 128]	2.556	40,636,466,453
Pruning Base Model	39,290	[1, 8, 16][16, 8, 32]	0.810	5,659,617,749
Student	7,766	[1, 2, 4][4, 2, 8]	0.441	1,003,700,933

3.1.1. Response-based Distillation

Leveraging the L2 and Kullback-Leibler (KL) divergence metrics, these functions measure the differences between the teacher and student network outputs. The student network endeavors to enhance its accuracy compared to the teacher by minimizing these error functions. Equations (2)

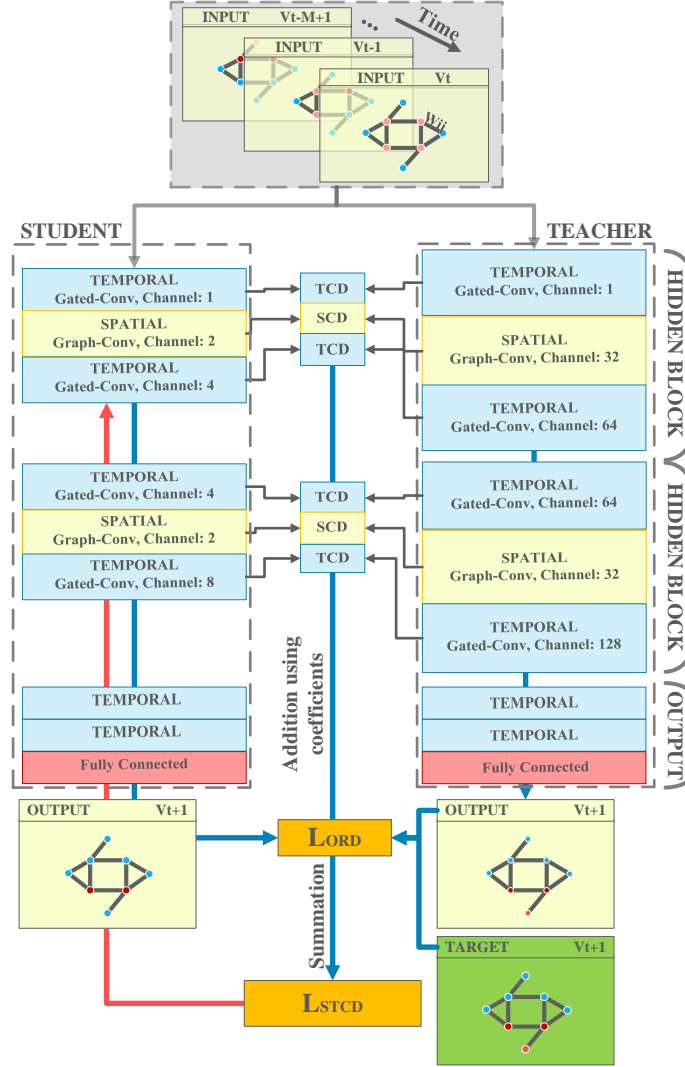


Figure 1: The illustration features both our student and teacher models, demonstrating the application of our cost functions to the spatio-temporal graph convolutional network (ST-GxCN)

and (3) employ the L2 and KL error functions to quantify the difference between the outputs of the teacher and student networks for each node.

$$\forall b \in B, \forall i \in N : \quad \text{KL}(y_{bi}^s, y_{bi}^t) = y_{bi}^t \log \left(\frac{y_{bi}^t}{y_{bi}^s} \right) \quad (1)$$

$$\forall b \in B, \forall i \in N : \quad L_{\text{RD(KL)bi}} = \beta \cdot \text{KL}(y_{bi}^s, y_{bi}^t) + (1 - \beta) \cdot \|y_{bi}^s - T_{bi}\|_2 \quad (2)$$

$$\forall b \in B, \forall i \in N : L_{RD(L2)bi} = \beta \cdot \|y_{bi}^s - y_{bi}^t\|_2 + (1 - \beta) \cdot \|y_{bi}^s - T_{bi}\|_2 \quad (3)$$

In these equations, $\|\cdot\|_2$ denotes the L2 norm. The variables N , y^s , and y^t represent the number of nodes, outputs of the student network, and outputs of the teacher network, respectively. KL is the Kullback-Leibler divergence metric (Equation (1)), T_{bi} is the target data value for batch b , and β is an adjustable coefficient. These cost functions consider both the teacher and target data jointly. However, we propose an alternative approach described by Equations (4) to (6) to determine when to use teacher predictions versus target data during student training. This decision hinges on the difference between teacher predictions and target data. If this difference exceeds a threshold (α_1), it indicates that even the more complex teacher model struggles to make an accurate prediction. In such cases, the simpler student model, with fewer parameters, is likely to face similar difficulties. Therefore, it is beneficial for the student to follow the teacher’s prediction, which tends to be smoother and less affected by noise. Otherwise, we use the target data directly. This method helps mitigate noise in the target data while leveraging the teacher’s more refined predictions to guide the student’s learning process effectively.

$$\forall b \in B, \forall i \in N : D_{bi}^t = |y_{bi}^t - T_{bi}| \quad (4)$$

$$D_{bi}^t = \frac{D_{bi}^t - \min(D_b^t)}{\max(D_b^t) - \min(D_b^t)} \quad (5)$$

$$L_{ORD+} = \sum_{b \in B} \sum_{i \in N} \begin{cases} \|y_{bi}^s - T_{bi}\|_2 & : D_{bi}^t \leq \alpha_1 \\ \|y_{bi}^s - y_{bi}^t\|_2 & : D_{bi}^t > \alpha_1 \end{cases} \quad (6)$$

In these equations, D_{bi}^t represents the absolute differences between teacher predictions and target data for each node in batch b . After normalization (Equation (5)), each element is compared with the threshold α_1 to identify potentially noisy data. The loss function L_{ORD} is then computed by summing these values for each node across all batches. You can observe the representation of this cost function in Figure 1.

3.1.2. Feature-based Knowledge Distillation in the Hidden Layers

Knowledge distillation from hidden layers simplifies the training process for deep and complex neural networks, making it less intricate and time-consuming. This method enables the training of simpler models that preserve meaningful information from the data and leverage the hidden

knowledge of more complex models. In the following subsections, we elaborate on our cost functions designed to capture both spatial and temporal correlations between the teacher and student networks. These cost functions aim to align the output of corresponding layers, fostering a close relationship in both spatial and temporal aspects.

Temporal Correlation Distillation We introduce the cost function L_{TCD} (as defined in equations (7) and (8) and illustrated in Figure 1) to ensure that the output of temporal layers in the student network closely aligns with the corresponding layers in the teacher network. The objective of L_{TCD} is to enable the temporal layers in the student network, which have fewer parameters compared to equivalent layers in the teacher network, to perform similarly.

$$TCD_{bnij} = \frac{1}{C} \sum_{c=1}^C |F_{binc} - F_{bjnc}|, \quad TCD \in \mathbb{R}^{B \times N \times T \times T} \quad (7)$$

$$L_{\text{TCD}} = \frac{1}{B \cdot N \cdot \binom{T}{2}} \sum_{b=1}^B \sum_{n=1}^N \sum_{\substack{i,j \\ j>i}}^T \|TCD_{bnij}^s - TCD_{bnij}^t\|_2 \quad (8)$$

In these equations, $F \in \mathbb{R}^{B \times T \times N \times C}$, where B is the batch size, T is the number of time steps, N is the number of graph nodes, and C is the number of channels. Each element of the TC tensor represents the absolute difference in features of a node at two time steps i and j . The cost function L_{TCD} addresses the difference in values for each node at two time steps. These errors are calculated using Equation (7) for both the teacher network and the student network. In the equation $\binom{T}{2}$, it accounts for the selection of any two time steps i and j out of T due to normalization. Finally, the difference between these two sets of Equations (8) yields the L_{TCD} cost function.

Spatial Correlation Distillation Assuming a resemblance between the output of a spatial layer and the temporal layers, the cost function computes pairwise differences in values for all nodes at each time step in both the student and teacher networks (see Equation (9)). These values are calculated for all spatial layers in both networks, and their pairwise differences are determined. To ensure a close alignment of the output from spatial layers in the student network with the corresponding layers in the teacher network, we introduce the cost function L_{SCD} , as defined in Equation (10) and illustrated in Figure 1.

$$SCD_{btij} = \frac{1}{C} \sum_{c=1}^C |F_{btic} - F_{btjc}|, \quad SCD \in \mathbb{R}^{B \times T \times N \times N} \quad (9)$$

$$L_{\text{SCD}} = \frac{1}{B \cdot T \cdot \binom{N}{2}} \sum_{b=1}^B \sum_{t=1}^T \sum_{\substack{i,j \\ j>i}}^N \|SCD_{btij}^s - SCD_{btij}^t\|_2 \quad (10)$$

Each element of the SC tensor represents the absolute difference in features of a node with another node at time step t . This tensor is computed for both the teacher and student networks (Equation (9)). The L_{SCD} cost function, calculated as the difference between these two vectors, is obtained from Equation (10).

3.1.3. Space-Time Cost Function

Through the integration of three distillation components, we construct a comprehensive cost function aimed at distilling relevant information pertaining to relationships within both temporal and spatial layers. The derived cost function is defined in Equation (11) and depicted in Figure 1.

$$L_{\text{STCD}} = L_{\text{ORD}} + \alpha_3 \cdot (\alpha_2 \cdot L_{\text{SCD}} + (1 - \alpha_2) \cdot L_{\text{TCD}}) \quad (11)$$

In this equation, the cost function L_{STCD} is a composite of three components. First we use L_{ORD} to address response distillation. In the feature-based area we use L_{SCD} and L_{TCD} to deal with spatial and temporal blocks in hidden layers. The parameters α_2 and α_3 allow adjusting the importance between temporal and spatial distillations and the significance given to distilling hidden layers in the cost function.

3.2. Pruning

In this subsection, we present an algorithm that employs the L_{STCD} cost function to train the student network. Additionally, it extracts the architecture of the student network by pruning insignificant parameters from the teacher network. The significance of each neuron is evaluated based on its influence on the network’s accuracy and its capacity to learn features extracted from the teacher. As outlined in the method presented by Molchanov et al. (2019), Equation (12) is utilized to establish a score I for a set of parameters labeled as w_s , similar to a convolutional filter. It is defined as a contribution to group sparsity in Equation (12):

$$I_S^{(1)}(W, B) \triangleq \sum_{s \in S} I_s^{(1)}(W, B) = \sum_{s \in S} \left(\sum_{i=1}^B (g_{s,i} w_{s,i})^2 \right) \quad (12)$$

In this paper, Equation (12) is used to obtain the importance score of parameters. However, instead of using the gradients and weights obtained from training the network in the standard form, the network is trained using cost function defined in the section 3.2. The importance score obtained from the gradients and weights of the network, this time, not only indicates the importance of the parameter in the output but also reflects the learning ability of the knowledge perceived and extracted by the teacher. The proposed method is outlined in Algorithm 1. The algorithm defines a mask matrix M to selectively retain or discard parameters in the network, with values of 1 or 0, respectively. An importance matrix **KDIS** is initialized to calculate the importance score of each parameter. The algorithm specifies minibatch intervals for pruning steps and the percentage of parameters to be pruned at each step. During each minibatch, the model undergoes fine-tuning using the L_{STCD} loss function (line 11), where gradients and importance scores (**KDIS**) are computed based on the network weights. Knowledge distillation (KD) is applied to calculate gradients and weights, denoted as **KDIS** instead of I . After a specified minibatch count in line 5, importance values are averaged, and parameters are pruned in each layer according to the specified percentage (lines 13 to 19). The pruned network is then fine-tuned over multiple epochs (lines 24 and 25). The resulting mask matrix M contains values of zero (removed parameters) and one (remaining parameters). Multiplying this matrix by the weight matrix of the student network’s base architecture yields the final pruned network.

4. Experiments and results

The results of traffic prediction in all tables are reported for the next 15, 30, and 45 minutes. The output values and calculated errors for these three time units are reported using three error functions: MAPE (Mean Absolute Percentage Error), MAE (Mean Absolute Error), and RMSE (Root Mean Square Error). The execution time reported in the tables are based on a batch of 1140 data and average over 100 runs. We thoroughly evaluate our model by testing it on two real traffic datasets: PeMSD7, which includes 228 nodes, and PeMSD8, with 170 nodes. **PeMSD7** is collected by over 39,000 sensor stations located throughout the main urban areas of the California state freeway system Yu et al. (2018). In this paper, we randomly select an average scale from Region 7 of California, consisting of 228 stations, labeled as PeMSD7. **PeMSD8** is similar to PeMSD7, with the difference that it includes traffic data for the city of San Bernardino from July to August 2016, collected from 170 monitoring stations on 8 streets at 5-minute intervals. All

Algorithm 1 Jointly KD-Pruning Algorithm

```
1: Input: base_model - Pre-trained model
2: Output: Pruned mask M
3: Initialize:
4: minibatch_counter  $\leftarrow$  0
5: pruning_minibatch  $\leftarrow$  your value here
6: KDIS  $\leftarrow$  Zero matrix with the shape of hidden block weights
7: M  $\leftarrow$  1 matrix with the shape of hidden block weights
8: pruning_percentage  $\leftarrow$   $n\%$ 
9: for each minibatch do
10:   minibatch_counter  $\leftarrow$  minibatch_counter + 1
11:   grads, weights  $\leftarrow$  Finetune(base_model,  $L_{\text{STCD}}$ , M)
12:   KDIS  $\leftarrow$  KDIS + compute_KDIS(grads, weights)
13:   if minibatch_counter == pruning_minibatch then
14:     minibatch_counter  $\leftarrow$  0
15:     KDIS  $\leftarrow$  KDIS / pruning_minibatch  $\triangleright$  Update pruning decision
16:     for each layer in layers do
17:       sort(KDIS[1], ASC)
18:       for each index in first_Npercent_indexes(KDIS) do
19:         M[1][p]  $\leftarrow$  0  $\triangleright$  Prune  $N\%$  of parameters with the lowest KDIS
20:       end for
21:     end for
22:   end if
23: end for
24: for several epochs do
25:   Finetune(base_model, ST-GCN, M)
26: end for
27: return M
```

presented results were generated using a TI 1080 GTX graphics card. We consistently used 12 historical timesteps M to predict 9 future timesteps H . Our model predicts these 9 timesteps sequentially, as illustrated in Figure 2. In this figure, each prediction (e.g., V_{t+1}) is utilized as the last graph in the input series to forecast the next timestep (V_{t+2}). This sequential approach enables us to predict h future timesteps. With data collected at 5-minute intervals, selecting 9 time units for prediction allows us to report results for the next 15, 30, and 45 minutes. Throughout all runs, the learning rate decreases by a factor of 0.7 after 5 epochs.

4.1. Hyperparameters

You can refer to Tables 2 for the learning rate, batch size, and hyperparameters related to knowledge distillation. In the context of the provided equations, the "Models" column enumerates various knowledge distillation approaches evaluated for PeMSD7 and PeMSD8 datasets. The hyperparameters $\alpha_1, \alpha_2, \alpha_3, \alpha$, and β are pivotal in the knowledge distillation process, as defined

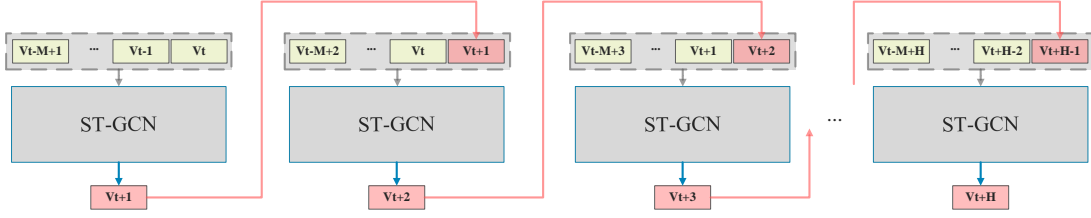


Figure 2: Sequence of ST-GCN predictions for future time steps. In each step, the output of the current state is used as the last input graph to predict the next timestep.

in equations (6), (11), (2), and (3). The hyperparameters for the proposed pruning algorithm are presented in Table 3. The table categorizes hyperparameters based on the percentage of pruning applied, as well as batch size, learning rate, and three alpha values (α_1 , α_2 , and α_3), specific to the PeMSD7 and PeMSD8 datasets. For instance, in the PeMSD7 row with a pruning percentage of 97%, only 3% of the model parameters are retained. The associated hyperparameters include a batch size of 25, a learning rate of 1×10^{-3} , and alpha values $\alpha_1 = 0.099$, $\alpha_2 = 0.091$, and $\alpha_3 = 0.531$.

Table 2: Hyperparameters of the proposed knowledge distillation loss functions

PeMSD7							
Models	Batch Size	Learning Rate	α_1	α_2	α_3	α	β
$L_{RD(L2)}$	50	1E-03	-	-	-	-	0.045
$L_{RD(KL)}$	50	1E-03	-	-	-	-	0.007
L_{SKD}	16	1E-03	-	-	-	0.333	-
$L_{ORD}(\text{ours})$	50	1E-03	0.593	-	-	-	-
$L_{STCD}(\text{ours})$	50	1E-03	0.170	0.047	0.313	-	-
PeMSD8							
Models	Batch Size	Learning Rate	α_1	α_2	α_3	α	β
$L_{RD(L2)}$	50	1E-03	-	-	-	-	0.905
$L_{RD(KL)}$	50	1E-03	-	-	-	-	0.728
L_{SKD}	60	1E-02	-	-	-	0.005	-
$L_{ORD}(\text{ours})$	50	1E-03	0.541	-	-	-	-
$L_{STCD}(\text{ours})$	50	1E-03	0.846	0.465	0.504	-	-

4.2. Knowledge Distillation Analysis

All knowledge distillation experiments, except for pruning, used the teacher and student models outlined in Table 1 and Figure 1. These models offer comprehensive information on both networks

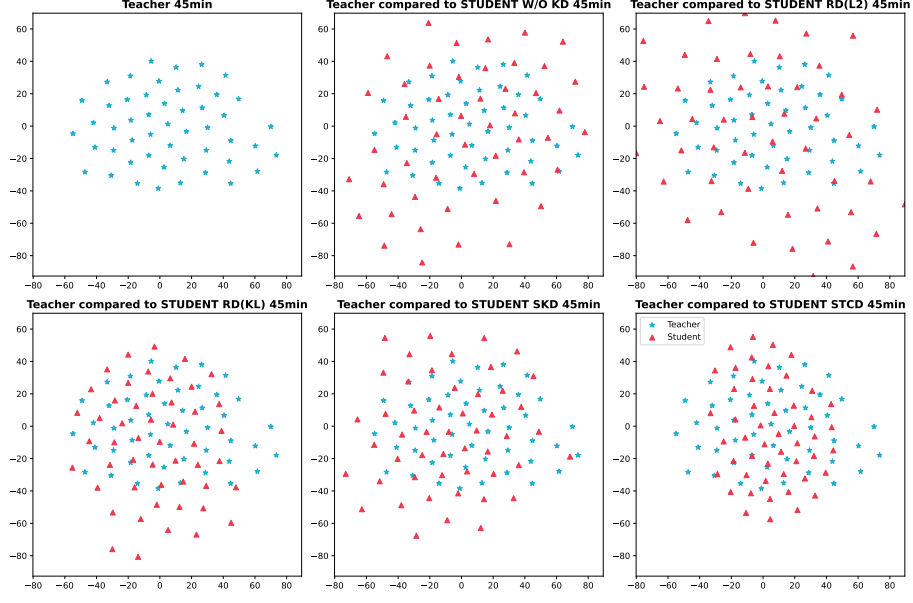
Table 3: Hyperparameters of the proposed pruning algorithm

PeMSD7						PeMSD8					
Pruned %	Batch Size	Learning Rate	α_1	α_2	α_3	Pruned %	Batch Size	Learning Rate	α_1	α_2	α_3
97%	25	1E-03	0.746	0.445	0.020	97%	25	1E-03	0.099	0.091	0.531
75%	50	1E-03	0.963	0.716	0.081	75%	50	1E-03	0.996	0.720	0.405
50%	50	1E-03	0.935	0.981	0.129	50%	50	1E-03	0.946	0.516	0.094
25%	50	1E-03	0.971	0.234	0.684	25%	50	1E-03	0.748	0.324	0.868

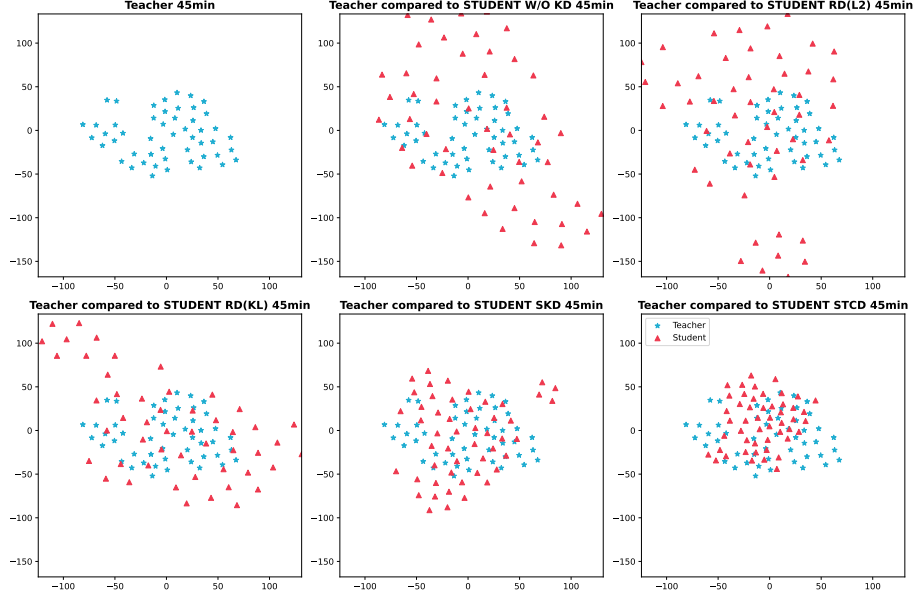
for easy comparison and analysis. The 'Hidden Blocks Channel' column in the table represents channels for spatial and temporal layers in the two hidden blocks of the ST-GCN network. These channels are visualized in the accompanying Figure. Additionally, 'Test Time (s)' denotes average test time over 100 trials, and 'FLOPS' indicates the network's floating-point operations per second (FLOPS) on a single forward pass. The student to teacher parameter ratio is approximately 3% in both datasets. The student network's execution time has decreased by around 83-84% compared to the teacher. Both networks have the same number of blocks and layers, with differences in parameter count due to variations in channel numbers per layer. The FLOPS ratio of the student network to the teacher is approximately 4% for the PeMSD7 dataset and 2.5% for the PeMSD8 dataset.

We conducted a comparative analysis of our final loss function, L_{STCD} , against several benchmarks: the baseline student model without knowledge distillation (KD), ARIMA, Historical Average, AST-GCNGuo et al. (2019); Li et al. (2021), and other established approaches Bian et al. (2021); Huang and Wang (2017); Zagoruyko and Komodakis (2016); Romero et al. (2014); Yang et al. (2020). The results are summarized in Table 4.

In reviewing the table, it is evident that for the PeMSD7 dataset, L_{STCD} consistently achieves lower Mean Absolute Error (MAE) and Root Mean Square Error (RMSE) for both 15-minute and 30-minute predictions. Similarly, on the PeMSD8 dataset, L_{STCD} demonstrates superior performance across various metrics when compared to $L_{RD(L_2)}$, $L_{RD(KL)}$, and L_{SKD} , as well as to lightweight models like ASTGCN. Figure 3 depict hidden layer representations for 50 test data points, with each point representing an individual instance. Red dots represent the student, while blue dots denote either the teacher or the baseline pruning network (utilized for specific pruning results). Proximity or overlap between red and blue dots serves as an indicator of the model's success. Ideally, effective methods show red and blue dots close to or overlapping each other. Figure 3 illustrates better convergence and pattern imitation of the L_{STCD} approach compared to other approaches in both knowledge bases.



(a) PeMSD7



(b) PeMSD8

Figure 3: Comparison of our spatial-temporal correlation distillation loss function L_{STCD} with the $L_{RD(L2)}$, $L_{RD(KL)}$ and L_{SKD} loss functions. Subfigure 3a shows results for PeMSD7 dataset, and Subfigure 3b shows for PeMSD8. The left chart in the top row corresponds to the teacher, while the middle chart in the top row pertains to a student without knowledge distillation. In the second row, the right chart represents our loss function, and the other charts indicate different loss functions.

Table 4: Comparison of our approach L_{STCD} with Historical Average, ARIMA, $L_{RD(L2)}$, $L_{RD(KL)}$ and L_{SKD} on PeMSD7 and PeMSD8

Models	PeMSD7								
	MAPE			MAE			RMSE		
	15 min	30 min	45 min	15 min	30 min	45 min	15 min	30 min	45 min
Teacher	5.223	7.316	8.739	2.230	3.010	3.565	4.097	5.752	6.834
HA	10.610			4.010			7.200		
ARIMA	13.400	14.010	15.010	5.570	5.940	6.270	9.000	9.220	9.430
ASTGCN	7.250	8.670	9.730	2.850	3.350	3.700	5.150	6.120	6.770
Student without KD	6.423	9.685	12.298	2.666	3.868	4.799	4.649	6.938	8.610
Student $L_{RD(L2)}$	6.379	9.661	12.474	2.768	4.214	5.527	4.709	7.185	9.178
Student $L_{RD(KL)}$	6.411	9.527	11.894	2.700	3.938	4.918	4.672	6.984	8.657
Student L_{SKD}	6.282	9.503	11.902	2.762	4.092	5.101	4.735	7.161	8.923
Student $L_{STCD}(ours)$	6.078	9.043	11.488	2.615	3.776	4.754	4.537	6.678	8.344

Models	PeMSD8								
	MAPE			MAE			RMSE		
	15 min	30 min	45 min	15 min	30 min	45 min	15 min	30 min	45 min
Teacher	2.293	3.239	3.925	1.211	1.665	2.031	2.524	3.501	4.081
HA	3.940			1.980			4.110		
ARIMA	5.110	5.210	5.460	1.900	2.120	2.430	4.870	5.240	5.630
ASTGCN	3.160	3.590	3.980	1.490	1.670	1.81	3.180	3.690	3.920
Student without KD	2.967	4.035	4.734	1.472	1.956	2.294	2.988	4.090	4.706
Student $L_{RD(L2)}$	2.812	3.976	4.908	1.426	1.953	2.387	2.839	3.978	4.733
Student $L_{RD(KL)}$	2.964	4.179	5.057	1.507	2.125	2.575	2.895	3.971	4.664
Student L_{SKD}	2.726	3.819	4.553	1.409	1.944	2.317	2.909	4.139	4.894
Student $L_{STCD}(ours)$	2.491	3.375	4.067	1.281	1.719	2.052	2.716	3.707	4.385

We also conducted an ablation study on our final loss function, L_{STCD} ; response-based distillation, L_{ORD} ; and other variants, including L_{TCD} , L_{SCD} , along with the baseline Student without KD (student trained without KD), and the findings are outlined in Table 5. Additionally, we report the ratio of attention to teacher output instead of the dataset target in Table 6.

4.3. Pruning and Fine-Tuning Analysis

In this section, the goal is to showcase that a consciously pruned student network, guided by Algorithm 1, exhibits superior learning capabilities compared to a predetermined student network

Table 5: Ablation study for our L_{STCD} loss function on PeMSD7 and PeMSD8

Models	PeMSD7								
	MAPE			MAE			RMSE		
	15 min	30 min	45 min	15 min	30 min	45 min	15 min	30 min	45 min
Teacher	5.223	7.316	8.739	2.230	3.010	3.565	4.097	5.752	6.834
Student without KD	6.423	9.685	12.298	2.666	3.868	4.799	4.649	6.938	8.610
Student L_{ORD}	6.411	9.516	12.104	2.762	4.091	5.221	4.645	6.847	8.569
Student L_{TCD}	6.320	9.411	11.667	2.730	3.966	4.853	4.678	6.899	8.512
Student L_{SCD}	6.326	9.193	11.380	2.743	3.957	4.866	4.645	6.853	8.476
Student L_{STCD}	6.078	9.043	11.488	2.615	3.776	4.754	4.537	6.678	8.344

Models	PeMSD8								
	MAPE			MAE			RMSE		
	15 min	30 min	45 min	15 min	30 min	45 min	15 min	30 min	45 min
Teacher	2.293	3.239	3.925	1.211	1.665	2.031	2.524	3.501	4.081
Student without KD	2.967	4.035	4.734	1.472	1.956	2.294	2.988	4.090	4.706
Student L_{ORD}	2.661	3.717	4.553	1.363	1.885	2.285	2.788	3.862	4.573
Student L_{TCD}	2.509	3.497	4.215	1.296	1.747	2.063	2.665	3.716	4.406
Student L_{SCD}	2.619	3.680	4.457	1.355	1.850	2.214	2.722	3.778	4.478
Student L_{STCD}	2.491	3.375	4.067	1.281	1.719	2.052	2.716	3.707	4.385

Table 6: Ratios of attention to teacher prediction to all training data

Models	Ratios of Attention to Teacher Prediction	
	PeMSD7	PeMSD8
Student L_{ORD}	3.009%	0.749%
Student L_{SCD}	1.377%	0.046%
Student L_{TCD}	64.637%	0.503%
Student L_{STCD}	15.844%	0.103%

used in knowledge distillation. The experiment’s outcomes are summarized in Table 7 and Figure 4. Table 7 presents results comparing the performance of the student network with and without pruning through knowledge distillation. Looking at the PeMSD7 dataset in the table, the teacher model, using all of its parameters, achieved an RMSE of 4.097 for a 15-minute prediction. On the other hand, the student model without the pruning algorithm, which retained about 3% of the parameters, had a higher RMSE of 4.537 for the same prediction period. However, when we applied the pruning algorithm to the student model (also retaining 3% of parameters), the RMSE improved

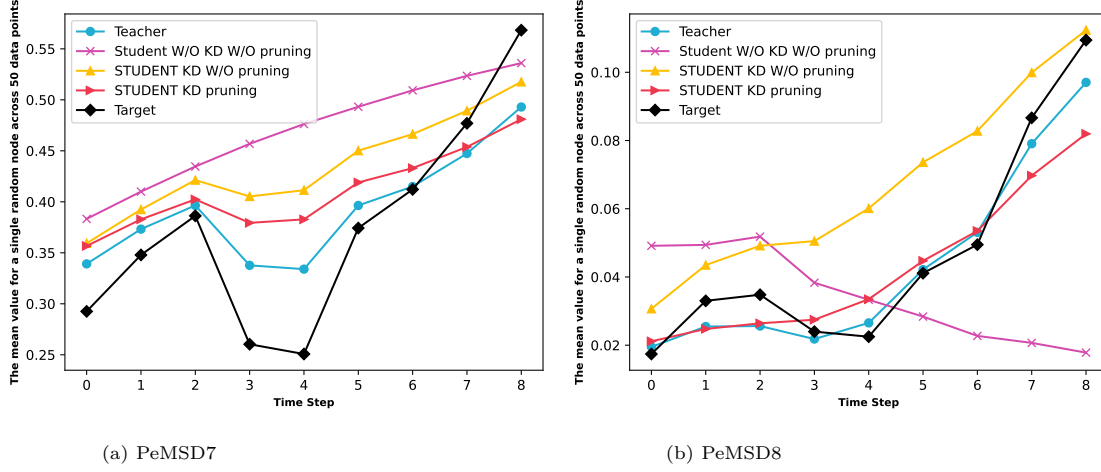


Figure 4: The results highlight the impact of employing the pruning algorithm, demonstrating the average predicted value for a randomly selected node based on 50 data points.

to 4.398. These results vividly demonstrate that the pruning algorithm significantly contributes to enhancing knowledge distillation, showcasing instances where pruning leads to better model performance compared to the non-pruned counterparts.

Table 7: The results showcase the impact of applying the pruning algorithm in enhancing knowledge distillation.

PeMSD7										
Models	Kept parameter %	MAPE			MAE			RMSE		
		15 min	30 min	45 min	15 min	30 min	45 min	15 min	30 min	45 min
Teacher	100%	5.223	7.316	8.739	2.230	3.010	3.565	4.097	5.752	6.834
Student without pruning algorithm	3%	6.078	9.043	11.488	2.615	3.776	4.754	4.537	6.678	8.344
Student with pruning algorithm	3%	5.691	8.410	10.520	2.470	3.366	4.131	4.264	6.152	7.564

PeMSD8										
Models	Kept parameter %	MAPE			MAE			RMSE		
		15 min	30 min	45 min	15 min	30 min	45 min	15 min	30 min	45 min
Teacher	100%	2.293	3.239	3.925	1.211	1.665	2.031	2.524	3.501	4.081
Student without pruning algorithm	3%	2.491	3.375	4.067	1.281	1.719	2.052	2.716	3.707	4.385
Student with pruning algorithm	3%	2.379	3.307	3.961	1.248	1.679	1.990	2.597	3.594	4.193

Previous research has confirmed that incorporating knowledge distillation enhances accuracy while utilizing a more straightforward model. Building upon this, our current study extends the concept, illustrating that Algorithm 1 yields a student architecture that performs better during training with

Table 8: Comparison of the performance between Algorithm 1 and the pruning algorithm that does not utilize knowledge distillation.

PeMSD7										
Models	Kept parameters %	MAPE			MAE			RMSE		
		15 min	30 min	45 min	15 min	30 min	45 min	15 min	30 min	45 min
Base Model	100%	5.512	8.004	9.988	2.321	3.216	3.896	4.177	6.006	7.341
Traditional pruning	75%	6.185	8.981	11.060	2.721	3.889	4.728	4.682	6.947	8.579
Pruned with L_{STCD} (ours)	75%	5.950	8.654	10.906	2.544	3.705	4.751	4.406	6.424	8.014
Traditional pruning	50%	6.571	9.735	12.114	2.975	4.389	5.418	4.858	7.255	8.971
Pruned with L_{STCD} (ours)	50%	6.232	9.185	11.419	2.584	3.773	4.723	4.524	6.773	8.448
Traditional pruning	25%	7.090	11.746	15.940	2.925	4.635	6.034	4.943	7.759	9.967
Pruned with L_{STCD} (ours)	25%	6.275	9.436	12.261	2.644	3.783	4.708	4.586	6.680	8.270

PeMSD8										
Models	Kept parameters %	MAPE			MAE			RMSE		
		15 min	30 min	45 min	15 min	30 min	45 min	15 min	30 min	45 min
Base Model	100%	2.206	3.028	3.677	1.187	1.592	1.924	2.479	3.434	4.084
Traditional pruning	75%	2.438	3.459	4.338	1.279	1.781	2.227	2.615	3.644	4.359
Pruned with L_{STCD} (ours)	75%	2.427	3.200	3.782	1.236	1.630	1.927	2.672	3.645	4.303
Traditional pruning	50%	2.456	3.514	4.449	1.322	1.890	2.397	2.648	3.797	4.685
Pruned with L_{STCD} (ours)	50%	2.424	3.310	3.988	1.261	1.693	2.029	2.605	3.550	4.169
Traditional pruning	25%	2.530	3.503	4.275	1.335	1.823	2.225	2.715	3.810	4.596
Pruned with L_{STCD} (ours)	25%	2.348	3.192	3.788	1.228	1.627	1.911	2.595	3.577	4.216

KD. We compare Algorithm 1 with Molchanov et al. (2019) using a base pruning model from Table 1 (second row). The results depicted in Table 8 underscore that our pruning algorithm consistently outperforms the alternative across various pruning percentages. Overall, the findings affirm that our introduced pruning algorithm plays a pivotal role in enhancing learning through knowledge distillation, significantly improving neural network accuracy by employing fewer parameters and simpler structures.

5. Conclusion and Future Works

5.1. Conclusion

We addressed the critical challenge of predicting traffic conditions to reduce transportation time. Our chosen methodology involved leveraging the spatio-temporal graph convolutional network (ST-GCN) for processing traffic prediction data, and we proposed a solution to improve the execution time of ST-GCNs. This involved introducing a novel approach that employed knowledge distillation to train a smaller network (referred to as the student) using distilled data from a more complex

network (referred to as the teacher), all while maintaining a high level of prediction accuracy. Additionally, we tackled the challenge of determining the architecture of the student network within the knowledge distillation process, employing Algorithm 1. Our findings demonstrated that a student network derived through Algorithm 1 exhibited enhanced performance during the knowledge distillation training process. Furthermore, by utilizing a simpler model in knowledge distillation, as opposed to the teacher model, as the base model in pruning, we illustrated that the performance of our algorithm was not necessarily contingent on the high accuracy of the base model. We evaluated our proposed concepts using two real-world datasets, PeMSD7 and PeMSD8, demonstrating the effectiveness of our approach in predicting traffic conditions. Overall, our research contributed to the field by presenting a methodology to optimize the execution time of spatio-temporal graph convolutional networks for traffic prediction without compromising accuracy.

5.2. Future Works

As we progress, we have the opportunity to explore our cost function L_{STCD} and Algorithm 1 on alternative spatiotemporal graph neural networks, such as ASTGCN. Furthermore, considering the method proposed in Luo et al. (2019) and Jing et al. (2021), we can explore whether using multiple teachers in Algorithm 1 and knowledge distillation with L_{STCD} can lead to a model with higher accuracy. Alternatively, we can develop a model capable of executing the tasks performed by all its teachers with increased accuracy and reduced execution time compared to the model in Jing et al. (2021). It is possible to enhance the concept of knowledge distillation based on the cost function L_{STCD} by incorporating relationship-based approaches. This improvement allows for the consideration of student and teacher networks with varying numbers of layers.

Additionally, improving the interpretability of distilled models can significantly increase trust and provide deeper insights into traffic patterns. Understanding how the student network makes its predictions can help identify potential improvements and uncover new traffic dynamics. For example, employing techniques like the ones proposed in Chen et al. (2023), which focus on enhancing the transparency of deep learning models, could be beneficial for our traffic prediction models.

Finally, developing advanced pruning techniques that consider structural properties of the network can lead to more efficient and compact models without sacrificing accuracy. By focusing on the importance of connections within the network, as seen in recent methods such as those described in Wang et al. (2023), we can achieve significant reductions in model complexity while maintaining

high performance. This approach aligns with our goal of optimizing the student network for real-time traffic prediction on resource-constrained devices.

In summary, future work can expand on our current framework by integrating adaptive learning mechanisms, improving model interpretability, and utilizing advanced pruning techniques, all of which will contribute to creating more robust and efficient traffic prediction models.

Declaration of Competing Interest

The authors declare that they have no known competing financial interests or personal relationships that could have appeared to influence the work reported in this paper.

Acknowledgements

This research did not receive any specific grant from funding agencies in the public, commercial, or not-for-profit sectors.

Data availability

Data will be made available on request.

Declaration of Generative AI and AI-assisted technologies in the writing process

During the preparation of this work the author(s) used ChatGPT 3.5 in order to refine language. After using this tool/service, the author(s) reviewed and edited the content as needed and take(s) full responsibility for the content of the publication.

References

Bing Yu, Haoteng Yin, and Zhanxing Zhu, *Spatio-Temporal Graph Convolutional Networks: A Deep Learning Framework for Traffic Forecasting*, Proceedings of the Twenty-Seventh International Joint Conference on Artificial Intelligence, 2018.

- David Alexander Tedjopurnomo, Zhifeng Bao, Baihua Zheng, Farhana Murtaza Choudhury, and A. K. Qin, *A Survey on Modern Deep Neural Network for Traffic Prediction: Trends, Methods and Challenges*, IEEE Transactions on Knowledge and Data Engineering, vol. 34, no. 4, pp. 1544-1561, 2022.
- Shengnan Guo, Yiqi Lin, Ning Feng, Chao Song, and Huaiyu Wan, *Attention Based Spatial-Temporal Graph Convolutional Networks for Traffic Flow Forecasting*, AAAI conference on artificial intelligence, 2019.
- Geoffrey Hinton, Oriol Vinyals, and Jeff Dean, *Distilling the knowledge in a neural network*, arXiv preprint arXiv:1503.02531, 2015.
- Yann LeCun, John Denker, and Sara Solla, *Optimal Brain Damage*, Advances in Neural Information Processing Systems, vol. 2, 1989.
- Pavlo Molchanov, Arun Mallya, Stephen Tyree, Iuri Frosio, and Jan Kautz, *Importance Estimation for Neural Network Pruning*, 2019 IEEE/CVF Conference on Computer Vision and Pattern Recognition (CVPR), pp. 11256-11264, 2019.
- Jianping Gou, Baosheng Yu, Stephen John Maybank, and Dacheng Tao, *Knowledge Distillation: A Survey*, International Journal of Computer Vision, 2021.
- Yu Cheng, Duo Wang, Pan Zhou, and Tao Zhang, *A Survey of Model Compression and Acceleration for Deep Neural Networks*, arXiv preprint arXiv:1710.09282, 2020.
- Junho Yim, Donggyu Joo, Jihoon Bae, and Junmo Kim, *A Gift from Knowledge Distillation: Fast Optimization, Network Minimization and Transfer Learning*, 2017 IEEE Conference on Computer Vision and Pattern Recognition (CVPR), pp. 7130-7138, 2017.
- Feng Zhang, Xiatian Zhu, and Mao Ye, *Fast human pose estimation*, Proceedings of the IEEE/CVF conference on computer vision and pattern recognition, pp. 3517-3526, 2019.
- Zhong Meng, Jinyu Li, Yong Zhao, and Yifan Gong, *Conditional Teacher-student Learning*, ICASSP 2019 - 2019 IEEE International Conference on Acoustics, Speech and Signal Processing (ICASSP), 2019.

- Peyman Passban, Yimeng Wu, Mehdi Rezagholizadeh, and Qun Liu, *Alp-kd: Attention-based layer projection for knowledge distillation*, Proceedings of the AAAI Conference on artificial intelligence, vol. 35, no. 15, pp. 13657-13665, 2021.
- Xiaobo Wang, Tianyu Fu, Shengcai Liao, Shuo Wang, Zhen Lei, and Tao Mei, *Exclusivity-Consistency Regularized Knowledge Distillation for Face Recognition*, Computer Vision – ECCV 2020, pp. 325-342, 2020.
- Umar Asif, Jianbin Tang, and Stefan Harrer, *Ensemble Knowledge Distillation for Learning Improved and Efficient Networks*, arXiv preprint arXiv:1909.08097, 2020.
- Seyed Iman Mirzadeh, Mehrdad Farajtabar, Ang Li, Nir Levine, Akihiro Matsukawa, and Hassan Ghasemzadeh, *Improved Knowledge Distillation via Teacher Assistant*, Proceedings of the AAAI Conference on Artificial Intelligence, vol. 34, no. 04, pp. 5191-5198, 2020.
- Hossein Mobahi, Mehrdad Farajtabar, and Peter Bartlett, *Self-Distillation Amplifies Regularization in Hilbert Space*, Advances in Neural Information Processing Systems, vol. 33, pp. 3351-3361, 2020.
- Wei Wen, Chunpeng Wu, Yandan Wang, Yiran Chen, and Hai Li, *Learning Structured Sparsity in Deep Neural Networks*, Advances in Neural Information Processing Systems, vol. 29, 2016.
- Xiang Li, Mengmeng Jiang, Bin Fan, and Liang Lin, *LSGCN: Long Short-Term Traffic Prediction with Graph Convolutional Networks*, IEEE Transactions on Intelligent Transportation Systems, vol. 22, no. 6, pp. 3535-3542, 2021.
- Nipun Ramakrishnan and Tarun Soni, *Network Traffic Prediction Using Recurrent Neural Networks*, 2018 17th IEEE International Conference on Machine Learning and Applications (ICMLA), pp. 187-193, 2018.
- Rusul L. Abduljabbar, Hussein Dia, and Pei-Wei Tsai, *Unidirectional and bidirectional LSTM models for short-term traffic prediction*, Journal of Advanced Transportation, pp. 1-16, 2021.
- Yiding Yang, Jiayan Qiu, Mingli Song, Dacheng Tao, and Xinchao Wang, *Distilling Knowledge From Graph Convolutional Networks*, Proceedings of the IEEE/CVF Conference on Computer Vision and Pattern Recognition (CVPR), June, 2020.

- Yongcheng Jing, Yiding Yang, Xinchao Wang, Mingli Song, and Dacheng Tao, *Amalgamating Knowledge from Heterogeneous Graph Neural Networks*, 2021 IEEE/CVF Conference on Computer Vision and Pattern Recognition (CVPR), pp. 15704-15713, 2021.
- Cunling Bian, Wei Feng, Liang Wan, and Song Wang, *Structural Knowledge Distillation for Efficient Skeleton-Based Action Recognition*, IEEE Transactions on Image Processing, vol. 30, pp. 2963-2976, 2021.
- Zehao Huang and Naiyan Wang, *Like what you like: Knowledge distill via neuron selectivity transfer*, arXiv preprint arXiv:1707.01219, 2017.
- Adriana Romero, Nicolas Ballas, Samira Ebrahimi Kahou, Antoine Chassang, Carlo Gatta, and Yoshua Bengio, *Fitnets: Hints for thin deep nets*, arXiv preprint arXiv:1412.6550, 2014.
- Sergey Zagoruyko and Nikos Komodakis, *Paying more attention to attention: Improving the performance of convolutional neural networks via attention transfer*, arXiv preprint arXiv:1612.03928, 2016.
- Cheng Yang, Jiawei Liu, and Chuan Shi, *Extract the Knowledge of Graph Neural Networks and Go Beyond it: An Effective Knowledge Distillation Framework*, Proceedings of the Web Conference 2021, pp. 1227-1237, 2021.
- Sihui Luo, Xinchao Wang, Gongfan Fang, Yao Hu, Dapeng Tao, and Mingli Song, *Knowledge Amalgamation from Heterogeneous Networks by Common Feature Learning*, Proceedings of the Twenty-Eighth International Joint Conference on Artificial Intelligence, IJCAI, Macao, China, August 10-16, 2019, pp. 3087-3093.
- Ying Li et al., *Deep knowledge distillation: A self-mutual learning framework for traffic prediction*, Expert Systems with Applications 252, 2024, p. 124138.
- Junzhong Ji, Fan Yu, and Minglong Lei, *Self-supervised spatiotemporal graph neural networks with self-distillation for traffic prediction*, IEEE Transactions on Intelligent Transportation Systems, vol. 24, no. 2, pp. 1580-1593, 2022.
- Hang Li et al., *Communication Traffic Prediction with Continual Knowledge Distillation*, ICC 2022-IEEE International Conference on Communications, 2022.

Weiwei Jiang and Jiayun Luo, *Graph neural network for traffic forecasting: A survey*, Expert Systems with Applications 207, 2022, p. 117921.

Weiwei Jiang et al., *Graph neural network for traffic forecasting: The research progress*, SPRS International Journal of Geo-Information 12.3, 2023, p. 100.

Xinyu Chen, Hui Zhang, and Jian Li, *Enhancing Transparency in Deep Learning Models for Traffic Prediction*, Journal of Advanced Transportation, 2023.

Yifan Wang, Lingling Xu, and Tao Zhou, *Structured Pruning of Graph Neural Networks for Efficient Inference*, IEEE Transactions on Neural Networks and Learning Systems, 2023.